

Porous silicon and siloxene: Vibrational and structural properties

H. D. Fuchs, M. Stutzmann, M. S. Brandt, M. Rosenbauer, J. Weber,
A. Breitschwerdt, P. Deák,* and M. Cardona

Max-Planck-Institut für Festkörperforschung, Heisenbergstrasse 1, D-70569 Stuttgart, Germany

(Received 17 February 1993)

Using Raman and infrared transmission spectroscopy, the vibrational properties of siloxene ($\text{Si}_6\text{O}_3\text{H}_6$) and its derivatives are investigated and interpreted in terms of various structural modifications of siloxene which have been proposed in the past. On the basis of experimental and theoretical investigations siloxene is found to be a mixture of Si_6 rings and/or linear Si chains interconnected by oxygen, and Si planes terminated by H and OH. The influence of thermal annealing, chemical treatment, and laser irradiation on the structure of siloxene is discussed in terms of the corresponding changes of the vibrational spectra and the x-ray-diffraction patterns. The vibrational properties of siloxene are very similar to those of electrochemically anodized porous Si. Raman, infrared transmission, and photoluminescence measurements of the two classes of materials are compared and a possible mechanism for the efficient luminescence in porous Si is discussed in light of the similarities between siloxene and porous Si.

I. INTRODUCTION

Silicon has been the dominant material for microelectronics for several decades. The technology and fabrication of Si-based electronic devices have been developed and refined in many ways and commercial applications now exist in a vast variety. However, in the past crystalline Si (*c*-Si) has never been a good candidate for active optoelectronic devices. The indirect energy gap of *c*-Si requires the participation of a phonon for the recombination of electrons and holes below 3.3 eV (to satisfy wave vector conservation), which makes optical recombinations in the visible spectrum rather weak. In order to realize optoelectronic applications within the well-known Si technology, the main approach has been to utilize the optical properties of III-V compounds such as GaAs or InP, leading to the wide field of heteroepitaxy on Si. Nevertheless, there still are efforts to overcome in Si the constraints imposed by wave vector conservation, e.g., by introducing point defects as radiative recombination centers, producing small Si crystallites with diameters small enough for significant quantum confinement (2–5 nm), or the fabrication of strained Si/Ge superlattices. As a simple guideline, the success which can be expected from such approaches depends critically on the overlap of the electronic wave functions of the states between which the optical transitions should occur. Even if the electronic wave function was localized within less than about ten lattice constants in two dimensions, the selection rules of the matrix elements would not be violated by more than 20% of a typical allowed matrix element, leading to transition probabilities of less than 4% of that of dipole-allowed transitions. Calculations of matrix elements M of the electron-hole-recombination yield $|M|^2=10^{-3}$ of allowed matrix elements for silicon crystallites with a diameter of ten lattice constants.¹ In tight

binding calculations, the crystallite size may not exceed about 8 Å for the transition matrix element to be comparable to direct materials (such as GaAs).² However, the photoluminescence efficiency of small crystallites may be enhanced with respect to the bulk due to a reduction of nonradiative recombination centers. In general, nonradiative recombination centers at the surfaces or heterointerfaces are a persistent problem in all approaches mentioned above.

There are several alloys of silicon with hydrogen, oxygen, and other elements which are known to exhibit a strong luminescence below 100 K, e.g., hydrogenated amorphous Si, *a*-Si:H, or its wide-band-gap alloys *a*-Si:O:H, *a*-Si:N:O:H, and *a*-Si:C:H. In Ref. 3 we have also compiled additional Si-related materials which have been reported to exhibit room temperature photoluminescence. Unfortunately, the luminescence in most cases is not strong enough for any practical applications.

About two years ago, Canham reported the observation of a strong photoluminescence (PL) in porous Si (*p*-Si) under UV illumination at 300 K.⁴ Independently, Lehmann and Gösele reported a pronounced shift of the fundamental absorption edge of self-supporting porous Si layers.⁵ Porous Si, obtained by electrochemical anodization of *c*-Si in electrolytes containing hydrofluoric (HF) acid, was first obtained in the 1950s during the study of electrolytic smoothing of Si surfaces (electropolishing),⁶ but it was not realized until 1990 that this material shows unexpected strong room temperature luminescence in the visible range.

Even though many groups have confirmed the existence of strongly luminescent *p*-Si layers, the origin and the mechanism of the luminescence remain controversial. The luminescence was first explained as a quantum-size effect in the “wirelike” pillars (diameter 2–3 nm) of the porous material.⁴ However, various researchers have noticed that there are several experimental results which

are not consistent with the concept of quantum confinement. Among those are the following.

(i) The fact that a similarly luminescent material can be obtained by anodic etching of amorphous Si instead of crystalline Si.⁷

(ii) The observed chemiluminescence in anodically and chemically etched porous Si.^{8,9}

(iii) The observed influence of a Bronsted or Lewis base on the luminescence properties of porous Si.^{10,11}

(iv) The slow photoluminescence decay after pulsed excitation (several orders of magnitude slower than in crystalline Si).^{12,13}

(v) The possibility of shifting the PL spectrum towards lower energies by chemical treatment of the samples (see discussion of Fig. 7 below).

(vi) The homogeneity of photoluminescence from the porous silicon samples (full width at half maximum of the PL spectra of about 350 meV) which would require a size distribution of the "wires" of only a few Angstrom.

(vii) The small fraction of 2–3 nm crystallites in *p*-Si which have been detected by electron microscopy, compared to the large external efficiency of the luminescence in *p*-Si of up to 10% and more at low temperatures.^{14,15}

Such experiments led to the idea that the luminescence might not be induced by the porous layer itself, which is certainly formed in all etch procedures, but that chemical substances produced during the etch, and mainly buried underneath or embedded inside the porous layer, might be the origin of the strong luminescence. Motohiro *et al.* suggested Si clusters connected with polysilane bridges, Prokes *et al.* favored (SiH₂) species, and our group proposed siloxene (Si₆O₃H₆) and its derivatives.^{12,16,17}

Siloxene and its derivatives have been known since 1863 and the remarkable luminescence behavior of this class of materials was first reported in 1922.^{18,19} Up to now, siloxene derivatives have been the only silicon-related compounds which are known to exhibit such strong room temperature photoluminescence. However, almost no work has been published dealing with the vibrational properties of siloxene, and the structure of the material is still controversial.^{12,19–21}

Vibrational spectroscopy is a very powerful tool for investigating the composition and structural properties of solids. In this work we compare the infrared transmission (IR) and Raman spectra of electrochemically prepared *p*-Si with those of chemically synthesized siloxene and its derivatives and correlate these results with the observed PL properties. The effect of thermal annealing, chemical treatment, and laser irradiation on the vibrational properties is discussed and compared to x-ray-diffraction and thermal effusion measurements performed on the same siloxene samples. The analysis of the experimental data provides evidence that siloxene derivatives, formed during the etching, are the structural origin of the strong luminescence in *p*-Si. The various structural configurations for siloxene (Si₆ rings, Si chains, Si planes) are discussed and related to the vibrational spectra. Our data suggest that *p*-Si as well as siloxene in general consist of a mixture of the ideal ring, plane, or chain configurations. Their relative contributions depend on the chemical and thermal treatment of the material.

II. SAMPLE PREPARATION AND EXPERIMENTAL DETAILS

We have prepared a large number of *p*-Si films using the standard electrochemical etch techniques in a solution of HF, H₂O, and ethanol. Many groups have reported detailed studies dealing with the influence of specific etching conditions on the porosity and the luminescence properties of such samples. The standard prescription which is easily reproduced is to start from *p*⁻ samples using low current densities and correspondingly long etch times. In contrast to these conditions, we have also been able to produce strongly luminescent *p*-Si samples from *p*⁺ or *n*⁺ Si and perform electrochemical treatment with very high current densities for short periods of time (several seconds to minutes). In the latter case, the Si wafer is usually covered by a black porous layer which does not exhibit any visible luminescence. Underneath this layer (which can be easily removed mechanically), however, a second layer appears which consists of a yellow material exhibiting the characteristics of a planar crystal structure (planes of yellow layers piled on top of each other). This second layer displays all luminescence properties usually ascribed to porous silicon.

In order to separate effects of the Si substrate from those of the etched part of the sample, we also fabricated self-supporting *p*-Si films, by complete anodic oxidation of 20- μ m-thick *p*⁺-doped Si wafers. For this method we used a simple setup where the Si wafer forms the anode of the electrolytic cell, and a piece of Pt metal the counterelectrode. For all samples we observed a characteristic sudden drop of the electrolytic current when the wafer was completely oxidized through,²² along with the formation of a self-supporting transparent, yellow/orange layer, similar to the material of the second layer underneath the porous material when the porous layer is formed on top of a thicker Si substrate. The self-supporting samples were then removed from the etch cell and air dried. Without further treatment, these samples showed strong orange photoluminescence, in particular at the edges.

All the measurements on *p*-Si shown in this work were performed on the self-supporting samples. This has to be taken into account when the results are compared to previous work by other authors. Some of the results reported recently may very well reflect the physical properties of the porous Si layer (Si skeleton), but might not be directly related to the origin of the PL. An indication of a basic problem in this respect is the fact that the Raman spectra of various *p*-Si samples which we have obtained from different groups vary considerably, but with no clear correlation to the observed PL. In Fig. 1 we show the Raman spectra, together with the corresponding PL spectra, of different siloxene and *p*-Si samples taken under identical conditions at room temperature with the 458-nm line of an Ar⁺-ion laser. Figure 2 gives the room temperature infrared transmission data of the same samples. The properties of the siloxene samples and also the details of the *p*-Si spectra will be discussed later. At this point we refer to Figs. 1 and 2 only to show that samples with comparable PL characteristics may display

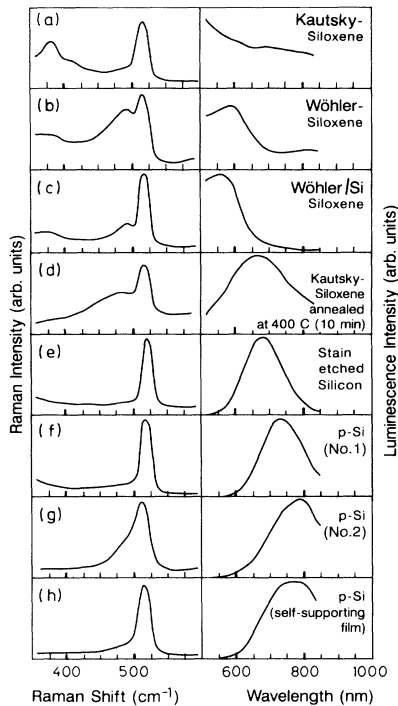


FIG. 1. Raman and photoluminescence spectra of various siloxene (a)–(d) and porous silicon (e)–(h) samples. The spectra were recorded under identical experimental conditions at 300 K with the 458-nm line of an Ar^+ laser. Note that the samples (d)–(h) exhibit comparable photoluminescence characteristics.

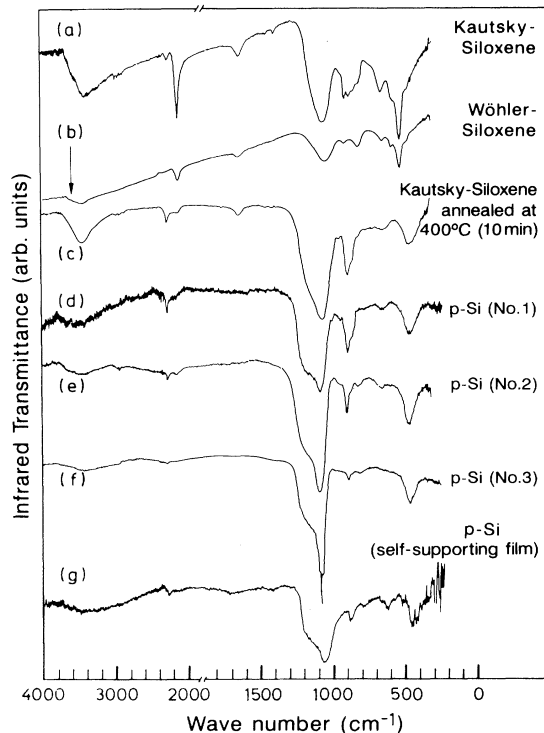


FIG. 2. Infrared transmittance spectra of various siloxene (a)–(c) and porous silicon (d)–(g) samples, recorded at 300 K. The samples (c)–(g) exhibit comparable photoluminescence characteristics.

quite different vibrational properties in Raman scattering [Figs. 1(d)–1(h)] but still exhibit a large number of common IR-absorption bands [Figs. 2(c)–2(g)]. We also have to keep in mind in this context that there are several Si-related structures which show room temperature PL, all of them, however, being at least two or three orders of magnitude less intense than *p*-Si or siloxene.³ Thus, if one compares weakly luminescent samples with typically 10%-efficient *p*-Si samples, conclusions from the observed vibrational properties should be made cautiously. As opposed to the porous Si layers, the Raman spectra of the strongly luminescent yellow material underneath the porous layer, as described above, are almost unaffected by changing the etching conditions.

To compare the optical properties of *p*-Si with those of synthesized siloxene we have prepared siloxene according to the recipes given in the related chemical literature.^{18,19} The starting material is a CaSi_2 powder (Johnson Matthey, tech. grade). CaSi_2 consists of alternating Ca layers and corrugated Si(111) planes.²³ The Ca is chemically removed in an HCl solution leaving the Si(111) planes basically intact and allowing for saturation of the remaining Si dangling bonds by H or OH. The details of this topochemical reaction depend on the chosen recipe. According to Wöhler,¹⁸ a 38% aqueous HCl solution has to be used. Later, Kautsky gave a more stringent recipe¹⁹ where ethanol is added to that solution, the temperature is kept at 0 °C, no oxygen or light is allowed during the chemical reaction, and the sample is washed after the process to remove the chlorine from the material. This completes the formation of siloxene. For further measurements the resulting siloxene was annealed at various temperatures.

An alternative method of producing luminescent siloxene on Si instead of using CaSi_2 powder, is to grow CaSi_2 on a Si wafer as a first step,²⁴ and then to use the same topochemical reaction as for the powder sample to transform CaSi_2 into siloxene.²⁵ This process is possible because the Si-Si bond lengths in CaSi_2 are only about 0.3% larger than in the (111) plane of *c*-Si.²⁰ Even the lattice spacing of siloxene is almost the same as in *c*-Si (within 0.5%),²⁰ which suggests that siloxene can be grown epitaxially on Si. Raman, IR, and photoluminescence measurements of such layers will be compared in this work to those of siloxene powder and *p*-Si.

The Raman spectra were recorded in backscattering geometry at various temperatures using different lines of an Ar^+ and a Kr^+ ion laser. The scattered light was dispersed by a double monochromator and the signal detected with conventional photon counting techniques. Extreme care had to be taken to avoid effects of intense laser illumination. Even an unfocused laser beam of only about 10 mW ($\approx 1 \text{ W/cm}^2$) was enough to affect the structure of the material and change the vibrational properties (see discussion below).²⁶ The PL as well as the Raman spectra were therefore recorded with laser intensities below 100 mW/cm². The PL signals were recorded with the same setup. For the direct comparison of the Raman and PL spectra on one sample, the setup was not changed between the respective measurements. All PL spectra shown in this work were corrected for the spec-

tral response of the detecting system.

The far-infrared transmission measurements were carried out on a NICOLET Fourier-transform spectrometer in the 300–4000-cm⁻¹ range. A He-cooled germanium bolometer was used as detector.

III. BASIC STRUCTURES OF SILOXENE

The synthesis of siloxene (Si₆O₃H₆) was described by Wöhler in 1863.¹⁸ Wöhler's recipe was refined later by Kautsky.¹⁹ Without direct experimental evidence, Kautsky proposed that siloxene consists of puckered sixfold Si rings interconnected by oxygen bridges. These Si₆ rings are the basic structural units already present in the Si(111) planes of CaSi₂ or crystalline Si but, according to Kautsky, in siloxene the Si₆ rings are separated by oxygen atoms inserted into the Si(111) plane. Thus, each Si atom is thought to be bonded to two other Si atoms and one oxygen. The remaining fourth valence of Si is saturated by hydrogen.¹⁹ A computer-generated structural model of these Si-ring structures is shown in Fig. 3(a).

About 60 years later, Weiss, Beil, and Meyer performed x-ray measurements on single crystals of siloxene and interpreted their data in terms of the structure shown in Fig. 3(c).²⁰ In this structure, the Si layers present in crystalline Si are essentially conserved, with a small decrease in the bond length (0.5%).²⁰ The planes are terminated by hydrogen and OH to form a graphitelike structure. Note, however, that the Si is fourfold coordinated (*sp*³) in all cases, as opposed to carbon which is *sp*² bonded in graphite.

Another possible form of siloxene [Fig. 3(b)] is an array

of linear Si chains interconnected by oxygen and terminated by hydrogen. This configuration could also be regarded as polysilane chains linked by oxygen bridges. It is interesting to note that the different configurations in Fig. 3 can be viewed as Si structures with increasing dimensionality: The "zero-dimensional" Si ring [Fig. 3(a)], the "one-dimensional" Si chains [Fig. 3(b)], and the "two-dimensional" Si planes [Fig. 3(c)]. In this context, we want to clarify the difference between *siloxane* and *siloxene*, which were sometimes confused in recent publications. The *siloxanes* are a class of compounds with Si-O-Si chains as the basic structural unit. There exist a large number of different linear, cyclic, and branched siloxanes with different lengths of the Si-O-Si chains and various chemical groups saturating the free valences.²⁷ *Siloxene* (Si₆O₃H₆) and its derivatives, on the other hand, consist basically of a Si skeleton (chains, rings, or planes), terminated and interconnected by various chemical groups.

Quantum chemical calculations of the three structures of siloxene shown in Fig. 3 have been performed, indicating that the layered structure [Fig. 3(c)] is only a metastable configuration.²⁸ The chain or the ring structure [Figs. 3(a) and 3(b)] both are lower in energy than the plane structure by about 1 eV per Si pair.²⁸

The three structures shown in Fig. 3 can be expected to have optical properties which are quite different from those of bulk crystalline Si. It has therefore been proposed that the striking luminescence properties of siloxene are a result of the presence of the Si₆ rings which act as molecular chromatophores in the material.¹⁹ It has already been reported in the early literature that a substitution of hydrogen by other monovalent radicals (e.g., OH, NH₂, CH₃O, Cl, etc.) changes the lumines-

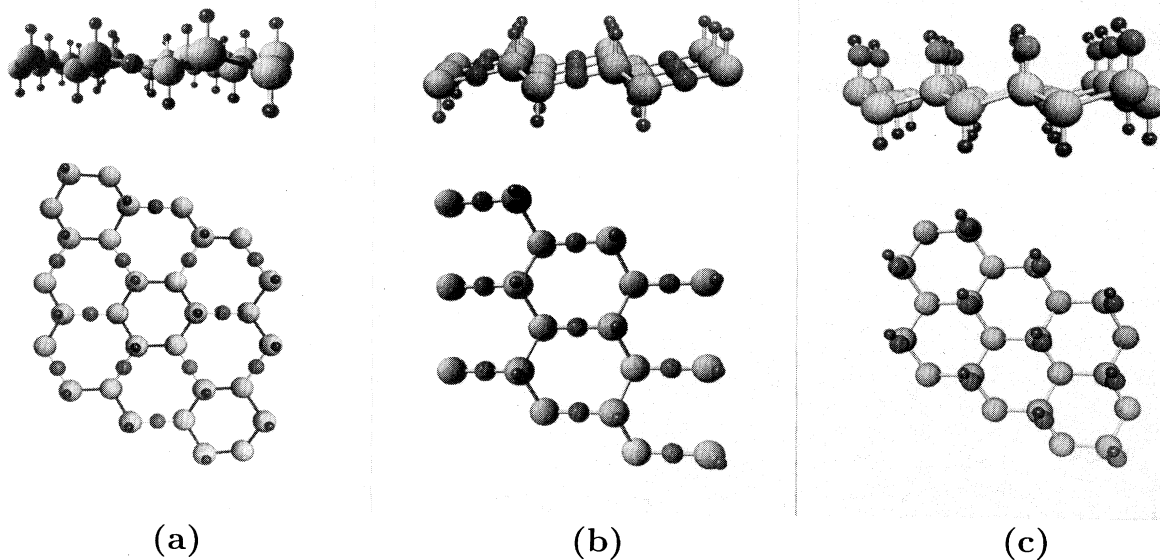


FIG. 3. Structural model of the different modifications of stoichiometric siloxene (Si₆O₃H₆): (a) Si₆ rings and (b) Si chains interconnected via oxygen bridges and terminated by hydrogen, (c) Si planes terminated by H and OH. Light atoms symbolize Si, small dark atoms hydrogen and larger dark atoms oxygen.

cence energy of siloxene in a characteristic manner, providing a means to tune the PL over most of the visible spectrum.^{29,30} A similar flexibility of the luminescence obtained from porous Si layers would be highly desirable in view of applications, but still remains to be demonstrated.

The vibrational properties of the ring structure [Fig. 3(a)] of siloxene have not been studied systematically in the past. Ubara *et al.* have interpreted their x-ray-diffraction, Raman, and IR spectra of annealed siloxene samples only in terms of the plane structure [Fig. 3(c)] and an amorphous phase.³¹ Polysilane, which is closely related to the chain structure of siloxene [Fig. 3(b)], has been investigated by various authors.^{32–38} Vora, Solin, and John have measured the Raman and infrared transmission spectra of polysilane as a function of the degree of oxidation³⁶ and their data are compared to the spectra of siloxene in the next section. Although polysilane also displays photoluminescence in the visible spectrum at room temperature, the vibrational spectra of polysilane and siloxene are drastically different (see Sec. IV). Furthermore, the efficiency of the luminescence in polysilane is more than an order of magnitude smaller than in siloxene or *p*-Si.^{15,34,35} It seems therefore unlikely that the chain structure of Fig. 3(b) contributes significantly to the luminescence of siloxene.

In the following section we will investigate the vibrational properties of siloxene in light of the various structural models (Fig. 3) and compare them to the results for *p*-Si. We will show that as-prepared Kautsky siloxene consists mainly of parallel Si(111) planes saturated by H and OH [Fig. 3(c)]. Such siloxene exhibits a blue-green luminescence and is unstable against heating or illumination in oxygen. Gentle heating leads to the insertion of oxygen (from the OH ligands) into the Si planes, fragmenting the Si planes and forming Si structures (Si₆ rings, etc.) which are isolated from each other by oxygen bridges. This annealed siloxene displays luminescence in the red and shows various properties similar to porous silicon. Intense illumination (above ≈ 1 W/cm²) or annealing above 400 °C destroys the luminescence of siloxene as well as porous silicon.

IV. EXPERIMENTAL RESULTS AND DISCUSSION

A. Raman experiments

As mentioned in Sec. II, siloxene (Si₆O₃H₆) is synthesized by a chemical transformation of CaSi₂ in HCl solution.^{18,19} Figure 4 compares the Raman spectra of the starting material CaSi₂ and the spectra of the resulting siloxene with the spectra of anodically etched porous Si (*p*-Si) and crystalline Si (*c*-Si). The spectra of the two strongly luminescent materials (*p*-Si and siloxene) in the vicinity of the Si-Si vibration of bulk *c*-Si show two distinct features: (i) The dominant Raman line is shifted towards lower energies by a few cm⁻¹ with respect to *c*-Si, and is slightly broadened. (ii) A weak and broad shoulder on the low-energy side appears in the spectra.

As mentioned in Sec. II, our Raman measurements

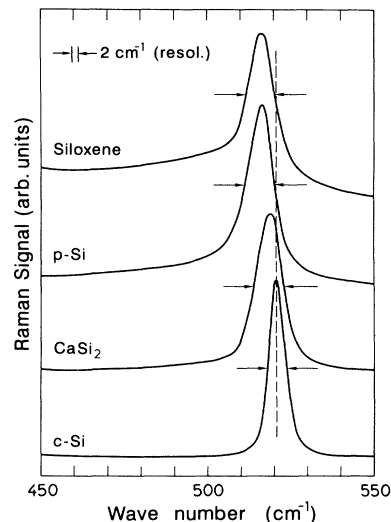


FIG. 4. Raman spectra of Kautsky siloxene, self-supporting porous silicon (*p*-Si), CaSi₂, and crystalline silicon (*c*-Si). The spectra were recorded under identical experimental conditions at 300 K with the 458-nm line of an Ar⁺ laser.

have not been performed on porous layers on substrates but on self-supporting layers which had been completely anodized. Otherwise, contributions of the remaining Si substrate have to be taken into account, which depend on the thickness and the effective absorption coefficient of the porous silicon layer. In general, such contributions are difficult to evaluate, in particular if one assumes that the thickness as well as the optical properties of porous Si can exhibit local fluctuations. For a correct experimental assessment of the phonon peak positions in *p*-Si it is therefore essential to remove the *p*-Si layer from the *c*-Si substrate not only to avoid the interference from the strong Raman phonons of the latter but also to prevent the buildup of macroscopic strain which could give rise to a shift of the Raman peak. In addition, great care has to be taken to rule out excessive heating of the *p*-Si layer whose thermal conductivity and heat capacity are much smaller than those of bulk Si because of the fractional topology.

The shift and slight broadening of the Si-Si Raman line at about 515 cm⁻¹ has been explained as a result of phonon confinement in the Si wires of *p*-Si produced during etching.^{39,40} More recently, Tsu, Shen, and Dutta interpreted the main Raman peak and the observed shoulder as a *k*-vector-induced TO-LO splitting in extremely small Si crystallites.⁴¹ Tsu, Shen, and Dutta caution, however, that “a simple momentum relaxation model” due to phonon confinement in the Si microstructures “does not predict this behavior,” because the induced TO phonon broadening would be larger than the TO-LO splitting which, in principle, should make it impossible to observe a resolved splitting.⁴¹

The effect of spatial confinement of phonons in small Si particles has been studied in the past both theoretically and experimentally.^{42,43} The breakdown of the *k*-selection rule leads to a broadening of the optical phonon

line. This broadening is correlated with a characteristic softening of the Raman modes, depending on the size and shape of the small particles. This is illustrated in Fig. 5, where the results of various groups for different sizes and shapes of Si particles have been compiled and compared to theoretical calculations. The calculations are based on the known phonon dispersion of bulk *c*-Si and describe the experimental data rather well.^{42,43} However, our experimental results for the optical phonons in *p*-Si, which are in general agreement with the work of Tsu, Shen, and Dutta,⁴¹ fall completely out of the region for microcrystalline Si. The shift of the Raman phonon in *p*-Si with respect to *c*-Si is about 6 cm^{-1} . This shift, according to Fig. 5, should be accompanied by a broadening of about 20 cm^{-1} in the case of spherical particles, and by an even larger broadening for the columnar structures which have been proposed as the origin of the PL in *p*-Si by Canham.⁴ The Raman spectra thus contradict the concept of Si wires of the order of 2–3 nm as being the main constituent of the luminescent material in *p*-Si. Furthermore, if the position and broadening of the Raman line of *p*-Si would reflect the quantum confinement in small Si wires, a direct correlation between the Raman and PL spectra would be expected. This is obviously not the case (see Fig. 1 and Ref. 44), a fact which suggests that the structures giving rise to the main Raman line might not be directly involved in the visible light emission.

The origin of the down-shifted Si-Si phonon in *p*-Si is illuminated by a comparison with the spectra of CaSi_2 whose structure consists of corrugated Si(111) planes separated by Ca layers. CaSi_2 shows a vibrational mode of the Si-planes which is very similar to that in *p*-Si (Fig. 4): The Raman line is shifted towards lower energies, but only slightly broadened. The Si planes of CaSi_2 are partially kept intact during the formation of siloxene, and the Raman spectrum of synthesized siloxene in Fig. 4 shows the corresponding mode. We therefore assign the

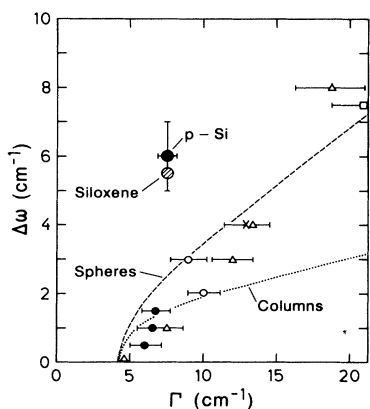


FIG. 5. Frequency shift of the Raman line from the position in crystalline silicon ($\Delta\omega$) vs full width at half maximum (Γ). Small symbols are experimental data for $\mu\text{c-Si}$ of various groups, large symbols experimental data for porous silicon and siloxene, and the dashed and dotted curves are theoretical calculations of Refs. 42 and 43.

mode at 515 cm^{-1} in *p*-Si to vibrations of the interconnected Si planes of siloxene.^{45,46} We note, however, that TEM micrographs indicate that the *p*-Si layers usually contain a certain fraction of larger Si crystallites with a size of typically 100 nm and above, depending on the etching conditions. These larger crystallites are expected to display Raman spectra similar to bulk Si. In fact, a closer look at the spectra in Fig. 4 shows that all spectra have some intensity on the high-energy shoulder of the peak around 520 cm^{-1} which allows for a possible contribution from those larger Si particles embedded in the *p*-Si layer. Compared to the bulk-Si phonons, however, the Raman response of siloxene might be enhanced with respect to bulk Si, e.g., due to resonances (the exciting laser energy is closer to the electronic gap of siloxene than to the one of *c*-Si) or absorption effects, which makes it impossible to observe the remaining Si particles in the *p*-Si layer as a separately resolved Raman line.

In Fig. 6 the spectra of siloxene, CaSi_2 , and *p*-Si are compared over an extended energy range. In addition to the 515- cm^{-1} mode, features around 380 cm^{-1} and 410 cm^{-1} appear in CaSi_2 and siloxene. Since these modes show up in both materials (together with the 515- cm^{-1} mode), and the only structures common to both are the corrugated Si(111) planes, we conclude that the Raman modes at 380 cm^{-1} , 410 cm^{-1} , and 515 cm^{-1} (Fig. 6) must originate from the Si planes in siloxene and CaSi_2 [Fig. 3(c)]. Similar modes have been obtained in calculations of the so-called bct5 structure of Si, which consists of sixfold Si rings perpendicular to the (110) planes with fivefold-coordinated Si.⁴⁷ Using local-density pseudopotential calculations, Raman-active phonons of the bct5 structures at 520 cm^{-1} (E_g symmetry) and 340 cm^{-1} (A_{1g} symmetry) were obtained, compared to

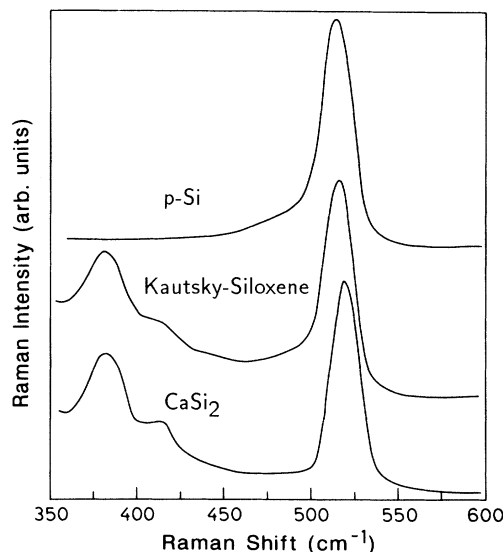


FIG. 6. Raman spectra of a self-supporting porous silicon film (*p*-Si), Kautsky siloxene, and CaSi_2 . The spectra were recorded under identical experimental conditions at 300 K with the 458-nm line of an Ar^+ laser. Note that the resolution of these spectra is five times higher than in Fig. 4.

521 cm^{-1} for *c*-Si.⁴⁷ The appearance of the additional lower-energy mode at 340 cm^{-1} in these calculations indicates that a breaking of the cubic symmetry of *c*-Si allows Raman modes below the one in *c*-Si, in the region where we observe the additional modes in siloxene and CaSi_2 (see also calculations below). The absence of a similar 380–410 cm^{-1} mode in *p*-Si (Fig. 6) will be discussed below in connection with the annealing experiments of siloxene.

More information about the structure of siloxene was obtained by annealing as-prepared material in air in steps of 100 °C and monitoring the changes in the IR and Raman spectra. In Fig. 7, the Raman results are shown together with the changes in the photoluminescence. The corresponding IR spectra will be discussed in Sec. IV B. The Raman spectra of siloxene prepared according to the stringent method described by Kautsky show a main peak at 515 cm^{-1} as discussed above, a shoulder on the low-energy side at around 495 cm^{-1} , and a structure at 380 cm^{-1} and 410 cm^{-1} . The 495- cm^{-1} shoulder rises to a clear peak when the sample is annealed for 10 min at about 100 °C. Annealing of the samples at higher temperatures leads to the emergence of a broader mode around 470 cm^{-1} which appears most clearly after annealing at 400 °C. Figure 7 also suggests that this 470- cm^{-1} Raman mode is directly related to the luminescence properties of the material: Whereas as-prepared Kautsky siloxene exhibits most of its PL in the green spectrum and only weak luminescence at lower energies, the PL of the 100 °C-annealed sample is shifted towards the red region of the spectrum, correlated with the appearance of the second peak in the Raman spectrum at 495 cm^{-1} . With increasing anneal temperature below 400 °C the 495- cm^{-1}

mode decreases and eventually merges with the broad 470- cm^{-1} band after 400 °C, accompanied by a continuously increasing PL signal. Annealing above 400 °C quenches the PL signal and the corresponding Raman modes.

As mentioned in Sec. III, there are several structural configurations which have been suggested for siloxene. The structural units according to Kautsky and Zocher are Si_6 rings interconnected via oxygen bridges [Fig. 3(a)],¹⁹ whereas Weiss, Beil, and Meyer suggested Si planes terminated by H and OH to be the structure of siloxene [Fig. 3(c)].²⁰ A third possible configuration is Si chains interconnected with oxygen bridges and terminated by hydrogen [Fig. 3(b)]. Currently, there is little theoretical or experimental data available concerning the Si-ring and Si-plane structure in siloxene. The chain structure, on the other hand, is similar to polysilane, as far as the Si-Si bonds are concerned, which has been investigated by Vora, Solin, and John.³⁶ They found four prominent Raman modes in polysilane: A broad band at 482 cm^{-1} with a width of 62 cm^{-1} (Si-Si vibration), and modes at 630 cm^{-1} (width 106 cm^{-1}), 909 cm^{-1} (width 45 cm^{-1}), and 2115 cm^{-1} (width 69 cm^{-1}) assigned to various Si-H vibrations.³⁶ Our data for *p*-Si and siloxene differ considerably from the spectra of polysilane (Fig. 6, see also discussion of Si-H and Si-O vibrations below), but it is not clear *a priori* how the presence of the oxygen bridges in the chain structure of siloxene would affect the vibrational modes compared to the pure polysilane.

Since the Si_6 rings seem to be the most likely candidates for inducing the PL in siloxene,^{12,29,30,48} the strong correlation between the PL intensity and the 470- cm^{-1} mode leads us to assign the 470- cm^{-1} mode to vibrations of those rings. The puckered Si_6 rings in siloxene belong to the point symmetry group D_{3d} .⁴⁹ The irreducible symmetry types (species) and characters for the D_{3d} point group are given in Table I. We have already discussed above the assignment of the 380–410- cm^{-1} modes and the 515- cm^{-1} mode as arising from the Si-plane structure in siloxene. The assignment of the 470 cm^{-1} to vibrations of the Si_6 rings is further supported by a recent theoretical analysis of the vibrational structure of siloxene. Deák *et al.* applied quantum chemical calculations (so-called AM1 calculations) to the various structural modifications of siloxene and obtained the corresponding vibrational modes.²⁸ They calculated the highest Si-Si stretching frequency in the ring structure of siloxene to be 469 cm^{-1} . In *p*-Si, this mode correlates with the low-energy shoulder in Fig. 4.

Complementary to the quantum chemical AM1 calculations we performed simple bond-bending, bond-stretching force constant calculations for the vibrational frequencies of the various configurations of siloxene. The calculations were done with the reasonable assumption that the force constants for the Si-Si stretching and bending vibrations in siloxene are the same as in bulk *c*-Si. The force constants $\alpha_{\text{Si-O}}$ for the Si-O bonds were estimated from the bond lengths l :

$$\frac{\alpha_{\text{Si-O}}}{\alpha_{\text{Si-Si}}} = \left(\frac{l_{\text{Si-Si}}}{l_{\text{Si-O}}} \right)^3 \approx 2. \quad (1)$$

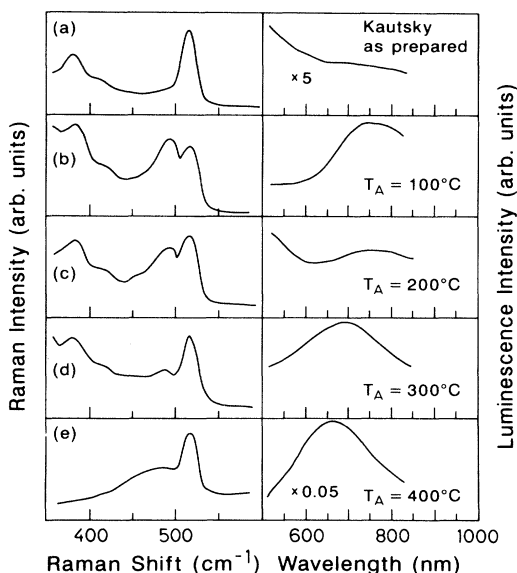


FIG. 7. Raman and photoluminescence spectra of as-prepared Kautsky siloxene (a), and after annealing at 100 °C, 200 °C, 300 °C, and 400 °C [(b)–(e)]. The measured spectra of (a) and (e) have been multiplied by the indicated factors before plotting. The spectra were recorded under identical experimental conditions at 300 K with the 458-nm line of an Ar^+ laser.

TABLE I. Symmetry types (species), characters, and selection rules for the point symmetry group D_{3d} .

	E	$2C_3$	$3C_2$	i	$2S_6$	$3\sigma_d$	Selection rules
A_{1g}	1	1	1	1	1	1	$\alpha_{xx} + \alpha_{yy}, \alpha_{zz}$
A_{1u}	1	1	1	-1	-1	-1	
A_{2g}	1	1	-1	1	1	-1	R_z
A_{2u}	1	1	-1	-1	-1	1	T_z
E_g	2	-1	0	2	-1	0	R_x, R_y $\alpha_{xx} - \alpha_{yy}, \alpha_{xy}$ α_{xz}, α_{yz}
E_u	2	-1	0	-2	1	0	T_x, T_y

The bond-bending force constant in c -Si is about one-third of that for stretching vibrations.⁵⁰ We assumed that this is also the case for the Si-Si and Si-O force constants in siloxene. To obtain the frequencies of the siloxene vibrational modes from the bulk Si-Si frequency (520 cm^{-1}), the contributions of the atomic displacements (Fig. 8) to the bond stretching and bending were added within a unit cell and compared to the corresponding contributions of c -Si. The ratio between c -Si and siloxene obtained in this way was used as a simple scaling factor for the phonon energies. In this simple approach we have also assumed that the Si-Si, the Si-H, and the Si-O vibrations are completely decoupled (adiabatic approximation). Even though most of the Si-O and Si-H vibrations are well separated in energy from the Si-Si vibrations, the decoupling of the modes is only a crude approximation, in particular for bending modes. This means, e.g., that the hydrogen atoms, not shown in Fig. 8, vibrate along with the Si atoms (piggyback), increasing the effective mass of the vibrating species (Si plus H). The results of these force constant calculations are shown in Fig. 8 for some of the Raman-active vibrations of the Si_6 rings and the Si planes of siloxene

together with the results of the quantum chemical calculations (AM1).

The bond-bending, bond-stretching considerations can also be used to calculate the Raman depolarization ratio $\rho = I_{\perp}/I_{\parallel}$, where I_{\perp} and I_{\parallel} denote the intensity of the depolarized and the polarized Raman spectra, respectively. In analogy with liquids or gases⁵¹ we can express the depolarization ratio ρ for randomly oriented particles (e.g., microcrystalline or amorphous Si) in terms of the components of the Raman tensor α_{ij} :

$$\rho = \frac{I_{\perp}}{I_{\parallel}} = \frac{3\beta^2}{45\alpha^2 + 4\beta^2}, \quad (2)$$

where

$$\alpha = \frac{1}{3} (\alpha_{xx} + \alpha_{yy} + \alpha_{zz}) \quad (3)$$

and

$$\beta^2 = \frac{1}{2} (\alpha_{xx} - \alpha_{yy})^2 + \frac{1}{2} (\alpha_{yy} - \alpha_{zz})^2 + \frac{1}{2} (\alpha_{zz} - \alpha_{xx})^2 + 3 (\alpha_{xy}^2 + \alpha_{yz}^2 + \alpha_{zx}^2). \quad (4)$$

Here α^2 and β^2 are the isotropic and anisotropic parts of the tensor, respectively. Expressed in terms of the polarizabilities parallel to the bonds (α_{\parallel}) and perpendicular to the bonds (α_{\perp}), α^2 and β^2 are in the case of a simple hexagonal two-dimensional lattice:

$$\alpha^2 = \left(\frac{\alpha_{\parallel} + 2\alpha_{\perp}}{2} \right)^2, \quad (5)$$

and

$$\beta^2 = 0.984 (\alpha_{\parallel} - \alpha_{\perp})^2. \quad (6)$$

For the limiting case of $\alpha_{\perp} = 0$ we find $\rho = 0.2$. If the values of c -Si from Ref. 52 ($\alpha_{\perp} = 52$, $\alpha_{\parallel} = 75$) are taken then $\rho = 0.004$. In our Raman experiments of p -Si, ρ is about 0.3. A detailed analysis of the depolarization ratio would also have to take into account other possible effects, such as surface enhanced Raman intensities, etc.

Siloxene compounds are not the only cyclic Si structures, but there is very little data available for Raman frequencies in other cyclic systems.²⁷ In Table II the observed Raman frequencies in p -Si and siloxene are compared to cyclic polysilane (Si_6H_{12}) (Ref. 27) and dimethylsiloxane ($[(\text{CH}_3)_2\text{SiO}]_x$).⁵³ This comparison is

Raman-active Si-Si Phonons in Siloxene

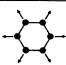
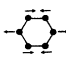
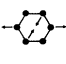
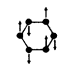
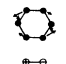
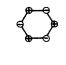

Si_6 - rings			Si-planes				
	Phonon frequency (cm^{-1})			Phonon frequency (cm^{-1})			
	Force constant model	AM1		Force constant model	AM1		
A_{1g}		480	469	E_g		480	478
E_g		450		E_g		480	
E_g		420		A_{1g}		≈ 150	
A_{1g}		≈ 150					

FIG. 8. Schematic of the Raman-active Si-Si vibrational modes in the Si_6 rings and the Si planes of siloxene (point symmetry group D_{3d}). The symmetry types, characters, and selection rules are given in Table I.

not done to give complete assignments but rather to show the trend of the observable Raman modes in such cyclic Si systems. Detailed vibrational calculations are clearly needed to clarify the origin of the various modes in the different siloxene modifications as well as in *p*-Si.

It is interesting to note in this context the observation of a mode around 488 cm^{-1} in amorphous *a*-SiO₂ (called "D₁ peak") (Ref. 54) which is similar to the one observed in siloxene, although it is not clear at this point if they really are related. In the case of *a*-SiO₂ this mode has been a matter of some controversy, but it is now commonly believed to arise from vibrations of planar threefold Si-O-Si rings.^{54,55} Fiori *et al.* claim to have produced such (Si-O)_{*n*} rings of different order *n* by irradiation of amorphous *a*-SiO₂ with UV light. The irradiated material was found to be luminescent in the red region of the spectrum after the rings were formed.^{56,57} The analogy between luminescence attributed to Si-O-Si rings in *a*-SiO₂ and Si₆ rings in siloxene, however, has to be handled with caution because there are other possible mechanisms for red luminescence in *a*-SiO₂.³

Our annealing experiments (Fig. 7), which are in general agreement with results for *p*-Si of Chen *et al.*⁵⁸ and Tsang, Tischler, and Collins⁴⁰ can be understood in light of the assignment mentioned above (see next section for the discussion of the corresponding IR spectra). Siloxene prepared according to the recipe of Kautsky consists mainly of Si planes terminated by H and OH radicals [Fig. 3(c)]. These Si planes are seen in the Raman spectra [Fig. 7(a)] as the structure around 380 cm^{-1} – 410 cm^{-1} and 515 cm^{-1} . Thermal oxidation of the planes leads to the insertion of O into the Si planes. The fragmentation of the Si planes by insertion of oxygen is indicated by the appearance of the Raman peak at 495 cm^{-1} in Fig. 7(b). The increasing fraction of oxygen in the Si planes with increasing anneal temperature below $400\text{ }^\circ\text{C}$ (annealed for 10 min in air) leads to the formation of Si₆ rings. This is seen in the Raman spectra [Figs. 7(b)–7(e)] as an increasing intensity of the 470 cm^{-1} mode, accompanied by the increase of the PL intensity by almost two orders of magnitude. The formation of the Si₆ rings is

probably followed by the substitution of H by OH as ligands. In this process, the structure corresponding to a PL peak energy at about 750 nm seems to be especially favored. It corresponds to approximately three hydrogen atoms per ring substituted by OH.²⁸ Above $400\text{ }^\circ\text{C}$, H is quickly evolved from the material and more oxygen is inserted into the Si planes, leaving behind a substoichiometric oxide, SiO_{*x*}, or oligomers such as the relatively stable (HSiO_{1.5})_{*n*} compounds.²⁷ The fact that the 470 cm^{-1} mode is drastically broadened for temperatures above $400\text{ }^\circ\text{C}$ indicates the formation of several types of Si-O-Si bonds. The 515 cm^{-1} mode does not disappear even at $400\text{ }^\circ\text{C}$, indicating that there are some Si-plane fragments withstanding the annealing, even though the Si rings are destroyed with the effusion of H. Furthermore, from the estimation of the frequencies of the Si rings given above, it cannot be excluded that the Si-ring structure also contributes somewhat to the Raman line at 515 cm^{-1} . If this were true, the 515 cm^{-1} mode might survive the structural change from Si planes to Si rings.

We have noted above the absence of the 380 – 410 cm^{-1} mode in *p*-Si in contrast to the CaSi₂ and the as-prepared Kautsky siloxene (Fig. 6). This is consistent with the analysis given above and can be explained as follows. The typical strong red/orange PL in the annealed siloxene samples, which is very similar to that of *p*-Si, stems from the Si₆ rings. The Si planes, which are responsible for the 380 – 410 cm^{-1} mode, on the other hand, lead to the green/yellow PL. If siloxene is the origin of the PL in *p*-Si then the similarity to the PL of the annealed siloxene samples suggests that mainly the Si₆-ring structure should be present in *p*-Si. The Raman spectra of *p*-Si indeed show no evidence of the presence of Si planes (no 380 – 410 cm^{-1} mode), but the low-energy shoulder of the main peak of *p*-Si in Fig. 6 resembles the 470 cm^{-1} mode from the Si₆ rings [Fig. 7(e)]. This is further supported by the IR spectra (see discussion below), where the spectra of *p*-Si are very similar to those of the annealed siloxene, rather than those of the as-prepared siloxene.

Note that the PL peak energy in Fig. 7 shifts to slightly higher energies as the anneal temperature in-

TABLE II. Raman-active vibrational modes of porous silicon and siloxene. For comparison, the experimental results of [(CH₃)₂SiO]₆ and Si₆H₁₂, as well as frequencies obtained from the quantum chemical AM1 calculations and the force constant model are also listed. All frequencies are given in units of cm^{-1} .

<i>p</i> -Si (exp.)	Siloxene (exp.)	[(CH ₃) ₂ SiO] ₆ (exp. Ref. 53)	Si ₆ H ₁₂ (exp. Ref. 27)	AM1 (calc. Ref. 28)	Force const. model (calc.)
	380		350 (Si-Si)		420
	410		455 (Si-Si)		450
	470		476 (Si-H)	469 (Si ring)	480
	495	493 (Si-O-Si)		478 (Si plane)	
515	515		515 (Si-H)	515 (Si-O-Si)	
620	635		655 (Si-H)		
	740		736 (Si-H)		
	900	872 (Si-O-Si)	893 (Si-H)		
960	975				
2130	2130		2128 (Si-H)	2105 (Si-H)	
2250	2150				

creases from 100 °C to 400 °C. Similar effects have been observed in the case of *p*-Si for thermal oxidation,⁵⁹ anodic oxidation,⁶⁰ and photo-oxidation.⁶¹ This PL energy shift has been explained within the quantum confinement model as arising from a reduction of the wire sizes.⁴ Calculations for siloxene, on the other hand,²⁸ show that shifts of the PL energy can be explained with changes in the electronic structure of siloxene as a result of a substitution of the Si-ring ligands. However, the exact reason for the upshift of the PL energy in the case of siloxene is presently not clear.

Insertion of oxygen into Si-backbone structures with resulting luminescence is also observed in other materials. Polysilane, e.g., shows an increase in room temperature luminescence due to oxidation.³⁶ Takagi *et al.* reported for μ c-Si that “photoluminescence could be seen in oxidized Si particles at room temperature by excitation with ultraviolet light, but cannot be seen in as-deposited samples.”⁶² Even though the photoluminescence in these cases does not have the same origin as in siloxene and the efficiency of the luminescence in these materials is several orders of magnitude less than in siloxene, oxygen again seems to be important to passivate recombination centers and to isolate the luminescent material from the surrounding material in order to create efficient radiative centers. Calculations of the electronic band structure of siloxene support the idea that oxygen acts as an insulator or spacer separating adjacent Si rings in siloxene.²⁸ In this (chemical) sense, the luminescence in siloxene can also be viewed as a spatial “confinement” effect.

Similar to thermal treatment (Fig. 7), strong laser illumination also changes the structure of siloxene (Fig. 9).²⁶ Illuminating the 100 °C-annealed siloxene sample for one hour with near-UV light ($\lambda_L = 413$ nm, 10 W/cm²) drastically reduces the fraction of Si rings in the material, seen in Fig. 9 as the decrease of the 470-cm⁻¹ and 495-cm⁻¹ modes with respect to the 515-cm⁻¹ mode. Simultaneously, the orange PL is reduced, leaving behind the green PL of the Si planes, similar to the PL of as-prepared Kautsky siloxene. Strong laser illumination seems to have an effect on siloxene similar to that of annealing above 400 °C: The Si skeleton is destroyed, probably through the effusion of hydrogen and subsequent oxidation. The remaining Si planes are relatively stable against photodesorption of hydrogen. Under cer-

tain experimental conditions (weak illumination, inert atmosphere, low temperature), the Si planes in particular appear to be relatively stable against light-induced structural changes. On the other hand, if the illumination is too strong (above ≈ 1 W/cm²) or the temperatures are too high (above ≈ 400 °C), the material is completely oxidized to α -SiO_x or structures such as (HSiO_{1.5})_n. This observation also applies to *p*-Si and shows how critical it is to control the incident laser intensity.^{26,63} Intense laser illumination can destroy the structure of *p*-Si during the measurement and quench the PL, which can be partially recovered by annealing or additional treatment with HF.^{15,26,63}

Tsang, Tischler, and Collins recently reported the change of the Raman spectra of *p*-Si as a function of thermal annealing and illumination.⁴⁰ They found that thermal treatment and laser irradiation change the Raman spectra in similar ways, and ascribed the broad feature in the spectra arising around 500 cm⁻¹ to additional Si-O bonds on the surface of the small Si crystallites in *p*-Si. An additional dip of the samples in an HF:water:ethanol solution partially recovered the original spectra by etching the oxidized part of the sample. Their results can easily be explained within the framework of our model. The Si planes fragmented by insertion of oxygen and presumably oxidized even further are quickly etched by the HF solution, leaving behind the remaining unoxidized parts of the siloxene. At the same time, it is obvious that the Si skeleton (Si not tied up in siloxene), which of course is present in the *p*-Si samples even if it is not responsible for the PL, is also oxidized by the treatment which oxidizes the siloxene, adding to the increasing density of Si-O bonds after the annealing. The HF then removes these Si oxides and passivates the surface with H.

This leads us to a more general observation: Treatments of the samples which change the Si skeleton in *p*-Si can also change the siloxene in the *p*-Si, and it is *a priori* not clear which of the two changes the PL. Since siloxene exhibits a very strong luminescence, only relatively small amounts of siloxene or siloxenelike structures in *p*-Si would be sufficient for the observed PL. Simply as a consequence of their relative fraction in the samples it might be easier to detect the changes of the Si skeleton experimentally, but that does not mean that these changes are responsible for the changes in the PL. This is the reason why we have studied the effects in pure siloxene in this work in order to discriminate among the various possibilities. In addition, siloxene is an interesting substance in its own right, independent of its role in the luminescence mechanism of porous Si.

Besides thermal treatment and intense illumination, the relative amounts of Si rings and planes also depend on the particular way in which the siloxene is obtained. Figures 1(a)–1(c) compare three types of siloxene obtained in different processes. The siloxene shown in Fig. 1(a) is synthesized according to Kautsky. As discussed above, only a small fraction of the material is found to be in the Si-ring-like structure. If the less stringent recipe of Wöhler is used [Fig. 1(b)], which, in particular, allows partial oxidation during preparation, Si rings are formed

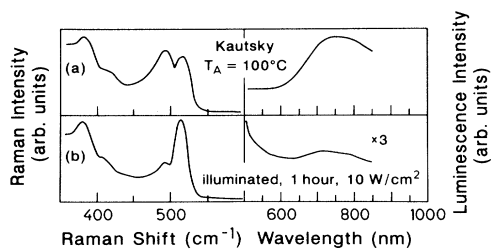


FIG. 9. Raman and photoluminescence spectra of (a) siloxene annealed at 100 °C (in order to obtain the red luminescence), and (b) after intense laser illumination. The spectra were recorded under identical experimental conditions at 300 K with the 458-nm line of an Ar⁺ laser.

similar to the case of thermal oxidation (Fig. 7). In siloxene formed from epitaxial CaSi_2 on Si [Fig. 1(c)], the formation of the rings is not as favorable as in CaSi_2 powder [Fig. 1(b)], probably because the presence of the Si surface of the wafer makes the Si-plane structure of siloxene more stable. Figures 1(a)–1(c) show again the close correlation between the 470-cm^{-1} – 495-cm^{-1} Raman modes (Si rings, fragmented Si planes) and the orange PL on the one side and between the 515-cm^{-1} mode (Si planes) and the green PL on the other side.

Raman scattering can also be used to study Si-H vibrations. This is shown in Fig. 10. Both siloxene and *p*-Si show Raman-active Si-H modes around 2130 cm^{-1} and 2250 cm^{-1} . The various vibrational modes of Si-H complexes as a function of annealing temperature will be further discussed in the next section based on the IR-transmission spectra. Here we just point out the striking similarity between the spectra of siloxene and *p*-Si, which leads to the conclusion that hydrogen is present in both materials in similar bonding configurations.

In Fig. 11, the second-order Raman spectra of Wöhler siloxene, *p*-Si, and *c*-Si are compared. It is well known that the two-phonon spectra of *c*-Si is dominated by contributions from phonons near the edge of the Brillouin zone where the phonon dispersion relation is flat, modified by momentum and symmetry selection rules. The main peak in the spectra of *c*-Si (Fig. 11) between 900 and 1000 cm^{-1} arises from processes involving two TO phonons, while the structure around 630 cm^{-1} stems from a combination of TO+TA phonons. Phonon confinement effects of the second-order spectra have been studied for $\mu\text{c-Si}$,⁶⁴ but the analysis is not as simple as in the case of the one-phonon spectra. Since the phonon energies are minimal at the zone edge, the relaxation of momentum conservation due to confinement of the phonons in the microcrystals should shift the peaks in the second-order spectra to higher energies as opposed to the first-order spectra where they are shifted downwards. One could even expect that the energy of the short-wavelength phonons from the zone edge may not be affected by the confinement at all. However, the experiments of Fauchet show a reduction of the peak

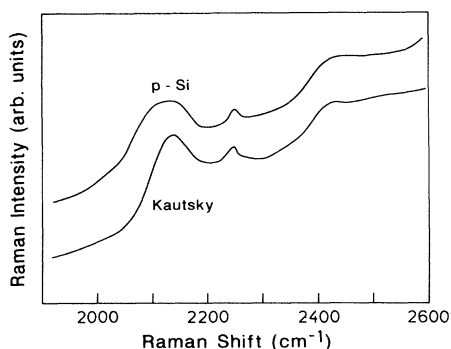


FIG. 10. Raman spectra of a self-supporting porous silicon film (*p*-Si) and Kautsky siloxene. The spectra were recorded under identical experimental conditions at 300 K with the 458-nm line of an Ar^+ laser.

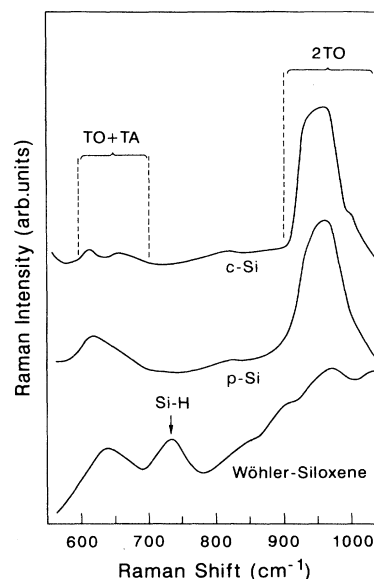


FIG. 11. Second-order Raman spectra of Wöhler siloxene, a self-supporting porous silicon film (*p*-Si) and crystalline silicon (*c*-Si). The spectra were recorded under identical experimental conditions at 300 K with the 458-nm line of an Ar^+ laser.

energies, accompanied by a broadening.⁶⁴ In addition, there is a relaxation of the symmetry selection rules for $\mu\text{c-Si}$ which allows stronger scattering around 630 cm^{-1} from (TO+TA) combinations.⁶⁴ Note that there are also Si-H bending modes in this frequency region which might contribute to the spectra of *p*-Si and siloxene. Because at present there is no model available to explain the second-order spectra of $\mu\text{c-Si}$, a detailed analysis of the spectra of siloxene and *p*-Si in Fig. 11 is not very meaningful, but an overall comparison with the corresponding spectra of Si nanocrystals with various crystallite sizes⁶⁴ complements the analysis of the first-order spectra. Comparing our data in Fig. 11 with those of Fauchet,⁶⁴ the spectra of our *p*-Si sample is basically identical to the spectra of Si crystals with a size of about 10 nm.⁶⁴ This is consistent with the analysis of the first-order spectra of *p*-Si given above which led to the conclusion that it is not impossible that some structures in the 2–3-nm range are present, but not as the main fraction of the sample.

The additional feature around 740 cm^{-1} in siloxene (Fig. 11) probably arises from two-phonon processes or from Si-H vibrations. In the cyclic polysilane Si_6H_{12} or the cyclotetrasiloxane $(\text{H}_2\text{SiO})_4$, e.g., the Raman spectra show Si-H vibrational modes at 736 cm^{-1} and 731 cm^{-1} , respectively.^{65,66} Similar vibrations could appear in siloxene but again, a detailed knowledge of the phonon modes in this class of materials would be necessary to unambiguously assign this mode.

B. Infrared transmission spectra

Complementary to the Raman measurements, we have performed infrared transmission spectroscopy on vari-

ous samples which show photoluminescence in the visible range of the spectrum: *p*-Si, different siloxene samples, and an amorphous *a*-Si:O:H sample with 30% O (Fig. 12). The siloxene annealed at 400 °C and the *p*-Si display an almost identical room temperature PL at about 750 nm.¹² In the *a*-Si:O:H sample, the luminescence is several orders of magnitude weaker and the peak is shifted towards the infrared.¹⁵ The IR spectra of the three typical samples shown in Fig. 12 are dominated by Si-O and Si-H vibrations (listed with the IR assignment in Table III). The relative intensities of these vibrational modes, however, are not the same for all three samples. While the IR spectra of *p*-Si and siloxene are almost identical over the entire frequency region from 300 cm⁻¹ to 4000 cm⁻¹, the intensities of the various modes in the amorphous *a*-Si:O:H are quite different.^{67,68} Considering the good agreement between the IR spectra of *p*-Si and siloxene, it can be concluded that Si, O, and H are present in similar bonding configurations.

There has been some controversy about whether as-prepared *p*-Si exhibits the oxygen-related IR bands immediately after the electrochemical etch or if these bands result from oxidation of the samples after removal from the etch solution.^{12,69} We will discuss the effects of ther-

TABLE III. Assignment of the infrared modes observed in porous silicon and siloxene.

ω (cm ⁻¹)	Assignment
460	Si-O-Si bending
520	Si-Si in Si planes
640	Si-H bending
706	O-Si-O bending
800	?
835	Si-H ₂ wagging
870	Si-H ₂ scissors
935	Si-O-Si bend stretching
962	?
1050–1150	Si-O-Si stretching
1620	O-H bending
2100	Si-H stretching
2200	O-Si-H stretching
2250	H-SiO ₃ stretching
3400–3580	O-H stretching

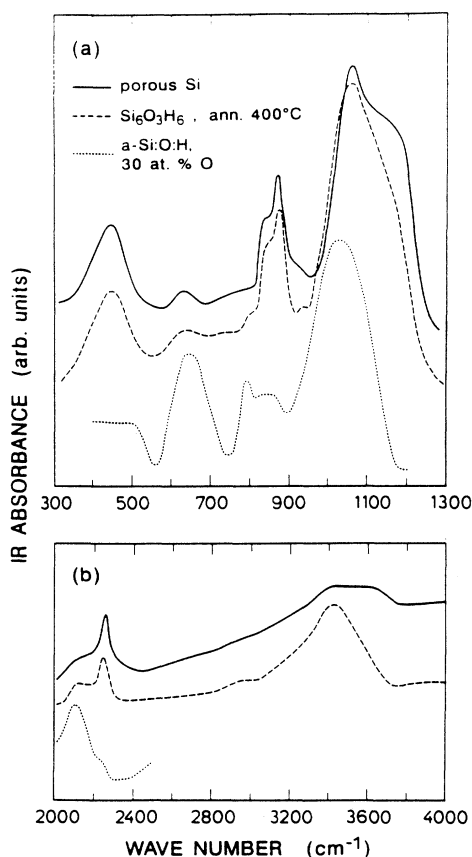


FIG. 12. Infrared absorption spectra of porous silicon (solid line), annealed siloxene (dashed line), and amorphous silicon alloy (dotted line). The assignment of the modes is discussed in the text and listed in Table III.

mal oxidation on the IR spectra of siloxene below in more detail. Nevertheless, we mention here that according to Refs. 70 and 69, aging of the *p*-Si samples in air leads to an increase of all the oxygen-related features in the spectra. However, all of the *p*-Si samples with a room temperature PL efficiency of about 10% which we have investigated showed the same oxygen-related bands in the IR spectra: the Si-O-Si bending vibrations at 460 cm⁻¹, the Si-O-Si stretching modes around 1050 cm⁻¹, the Si-H stretching modes at frequencies around 2250 cm⁻¹ which are characteristic for Si-H vibrations where O is backbonded to the Si, and the OH modes around 3400 cm⁻¹. We emphasize that the *p*-Si samples used in our experiments are all in the 10% PL-efficiency range. This is important when comparing their IR spectra to spectra of other groups. If the luminescence in a sample is less by a factor of 10 or 100, it could still be easily detected, while the oxygen or hydrogen content (which seems to be directly related to the PL intensity) might be well below the detection limit of IR measurements. Thus, as mentioned above in the context of Raman spectroscopy on *p*-Si, a meaningful comparison of the IR spectra is only possible when scaled with respect to the absolute PL efficiencies.

The dominant Si-O-Si stretching vibration, which has a two-peak structure in *p*-Si and siloxene (1050 cm⁻¹ and 1170 cm⁻¹), gives rise to only a single lower-frequency peak in *a*-Si:O:H (1020 cm⁻¹). An interesting analogy to the double-peak structure in siloxene is a similar behavior observed in the IR spectra of cyclic, branched, and linear methyl siloxanes.⁷¹ Wright and Hunter observed a split of the IR Si-O-Si band around 1100 cm⁻¹ into two peaks in the case of higher-order cyclosiloxanes, a split into three peaks for linear siloxanes, and no split at all in the randomly branched siloxanes.⁷¹ The conclusion is that the ordering of oxygen atoms in the structure of the siloxanes leads to a split of the Si-O-Si vibrational band. Since the ordering of the Si-O-Si bridges in the Si₆-ring structure of siloxene is similar to that in the cyclic siloxanes, it is possible that the splitting of the IR band in

siloxene has a similar origin: the periodic formation of the interconnecting Si-O-Si bridges. It is interesting that the IR spectra of *p*-Si in Fig. 12 exhibit a similar splitting of the Si-O-Si band, in agreement with the results of other groups.⁷⁰ This splitting could be caused either by a mechanism similar to the one in siloxene (ordering of Si-O-Si bridges) or by the presence of two different types of Si-O-Si bonds in the material. Candidates for the latter case are SiO₂ precipitates (Si-O-Si stretching vibration at 1100 cm⁻¹) and interstitial oxygen (Si-O-Si stretching vibration at about 1050 cm⁻¹). One way to distinguish the two possibilities is their behavior upon thermal annealing. At temperatures above 500 °C (annealing for about 10 min) most of the Si₆ rings of siloxene are destroyed (see discussion below), leading to the appearance of only one Si-O-Si mode. Such an annealing, on the other hand, should not allow the interstitial oxygen to merge with the precipitates, resulting in the two-peak structure even for anneal temperatures as high as 500 °C. In annealing experiments with *p*-Si, however, other effects of the thermal treatment, such as the formation of various defects, also have to be taken into account. Therefore, the presently available experimental results are not conclusive.

As mentioned above, in the course of the experiments described here, luminescent siloxene has not only been synthesized as a powder but has also been grown as a thin film on a Si wafer via the growth of CaSi₂ on Si.²⁵ The PL of such siloxene is shifted towards the green, presumably due to a preferred formation of Si planes rather than Si rings. The IR spectrum of siloxene grown on a Si wafer is compared to that of siloxene from CaSi₂ powder in Fig. 13(a), and for better reference their relative PL signals are shown in Fig. 13(b) (the PL of the annealed siloxene and of *p*-Si are also shown for comparison). The IR spectra of the powder siloxene and the siloxene grown on Si are almost identical, showing that it is indeed possible to grow siloxene on Si in this way.²⁵

In order to shed more light on the thermally induced structural changes in siloxene already discussed above, we have also followed the changes of the IR spectra caused by annealing in air (10 min at each respective temperature). The resulting IR spectra for siloxene prepared according to the recipe of Kautsky are shown in Fig. 14. The spectra of the as-prepared Kautsky siloxene sample, like those of the Wöhler siloxene of Figs. 12 and 14, are dominated by the Si-O-Si stretch vibration around 1100 cm⁻¹, the sharp Si-H stretch vibrational band at 2100 cm⁻¹, and various Si-H and Si-O bands between 650 cm⁻¹ and 900 cm⁻¹ (see Table III for details). Besides these localized modes there is a sharp feature at 520 cm⁻¹. One possible assignment for this mode is a Si-O vibration,⁷² but in our case its intensity decreases with increasing oxygen content, which speaks against that conjecture. Instead, we assign this 520-cm⁻¹ mode to the same origin as the corresponding Raman line at 515 cm⁻¹ (see above): optical phonons confined within the Si planes of siloxene. In a nonpolar material such as Si these phonons would usually not be observable in IR but they become infrared active because a dipole moment is induced due to the different electronegativity of the Si ligands (H, OH, ...). This characteristic mode of as-prepared Kaut-

sky siloxene is quenched upon annealing and disappears for anneal temperatures above 400 °C. Ubara *et al.* have reported the same evolution of the intensity of the 520-cm⁻¹ mode as a function of the anneal temperature.³¹ However, they did not discuss the physical origin of this mode.

The thermal behavior of the IR spectra of siloxene (Fig. 14) can be explained with the same structural changes in siloxene upon annealing that were indicated by the Raman spectra (Fig. 7): The metastable Si planes (520 cm⁻¹-mode) are partially destroyed by inserting oxygen into the planes to form the Si rings. As a result, the Si-O-Si stretch vibrations around 1100 cm⁻¹

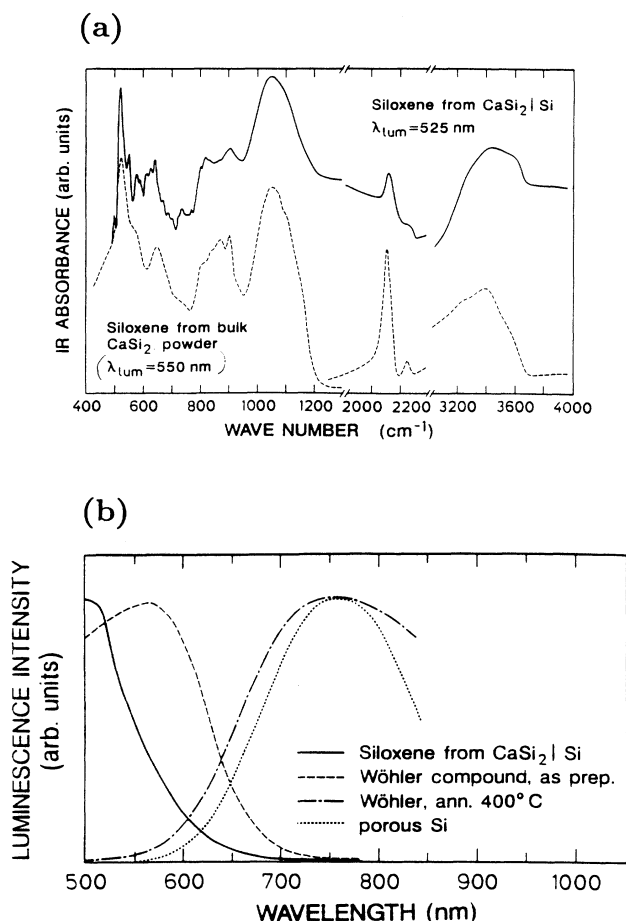


FIG. 13. (a) Comparison of the infrared absorption spectra of siloxene produced from a layer of CaSi₂ grown on crystalline silicon (solid line) and from CaSi₂ powder (dashed line), demonstrating that thin siloxene layers can be grown on crystalline silicon by the method described in the text. (λ_{lum} is the position of the maximum of the observed luminescence.) (b) Comparison of the corresponding photoluminescence spectra, together with the ones from an annealed Wöhler siloxene and a porous silicon sample. Note that the intensity of the siloxene film is about a factor of 5 higher than the luminescence of the porous silicon sample. The spectra were recorded under identical experimental conditions at 300 K with the 458-nm line of an Ar⁺ laser.

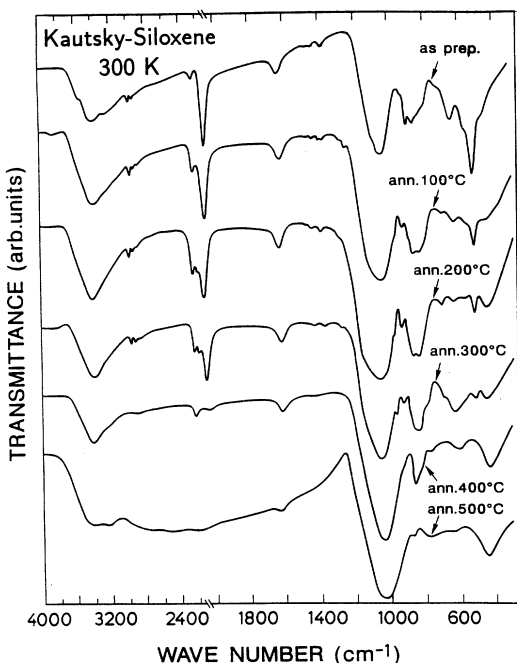


FIG. 14. Infrared transmittance spectra of siloxene at 300 K. The upper trace shows the spectrum of an as-prepared sample. The following spectra were obtained after annealing in air at the indicated temperatures.

and the Si-O-Si bending vibrations at 460 cm^{-1} in the IR spectra increase in strength. These structural changes are further corroborated by a comparison of the x-ray-diffraction patterns of as-prepared siloxene and an annealed sample, as shown in Fig. 15. Note that the sharp peaks in the pattern of Fig. 15 (marked with *) at diffraction angles (2θ) of 28.4° , 30.0° , 47.0° , 56.3° , 58.9° , 69.1° , and 76.1° arise from randomly oriented Si crystals (size of several μm) present in the samples which stem from impurities in the CaSi_2 powder used for the synthesis of the siloxene. The Si crystallites are unaffected by the thermal annealing at 400°C and the corresponding peaks also appear in the x-ray pattern of the annealed sample. Previously, Weiss, Beil, and Meyer have performed a study of the x-ray-diffraction patterns of siloxene samples prepared under various conditions.²⁰ They found that the Si-Si bond length within the Si planes of siloxene [Fig. 3(c)] is changed only slightly with respect to crystalline Si (-0.5%), corresponding to the peaks close to or superimposed on the Si-crystallite peaks in Fig. 15. The spacing between adjacent Si layers in siloxene, on the other hand, can be varied significantly by substituting H and OH by other ligands (intercalation).²⁰ The basal spacing between the Si layers is 0.63 nm for the pure as-prepared siloxene,^{20,31} seen as the peak around 14° in the spectra of Fig. 15. Ubara *et al.* have monitored the intensity of this 14° peak as a function of the anneal temperature,³¹ and found that it decreases with increasing anneal temperature. After annealing the sample at 400°C , the 14° peak, which is an indication of the existence of ordered Si planes in siloxene, completely disappears (lower trace in Fig. 15), and a broad background

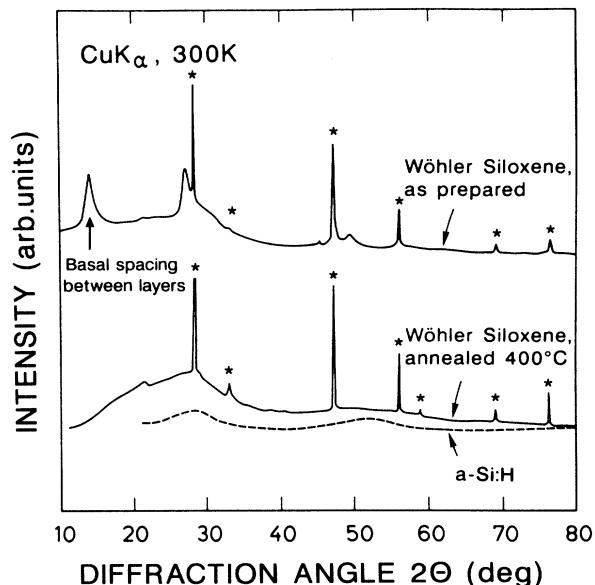


FIG. 15. X-ray-diffraction pattern of as-prepared Wöhler siloxene (upper trace) and the same sample after annealing at 400°C (lower trace, solid curve). The pattern of hydrogenated amorphous silicon is shown for comparison (dashed curve). The sharp peaks labeled with * arise from randomly oriented Si microcrystals in siloxene which stem from impurities in the CaSi_2 powder used for the synthesis.

similar to the diffraction pattern of amorphous silicon (also shown in Fig. 15) appears in addition to the $\mu\text{c-Si}$ peaks. The disappearance of the 14° peak, analogous to the disappearance of the 520-cm^{-1} mode in the IR spectra, is an indication of the amorphization of siloxene caused by the temperature-activated insertion of oxygen into the Si planes. The transformation due to annealing of siloxene from the Si-plane structure [Fig. 3(c)] to either the Si-chain structure [Fig. 3(b)] or the Si_6 rings [Fig. 3(a)] seems not to be selective or complete. The x-ray pattern of the annealed sample in Fig. 15 suggests, rather, a random mixture of possibly all three phases.

The insertion of oxygen into the Si-Si bonds can also be seen in the development of the Si-H vibrations between 2100 and 2250 cm^{-1} . As-prepared siloxene displays a sharp feature at 2100 cm^{-1} , which has been observed before on H-terminated Si(111) surfaces⁷³ and is known to arise from Si-H stretch vibrations. Oxygen on the back bond of a Si atom bound to hydrogen increases the Si-H vibrational frequency, and with increasing anneal temperature two distinct side bands arise at 2200 and 2250 cm^{-1} . Furthermore, additional modes, also related to the increasing oxygen content, appear at 706 , 928 , and 962 cm^{-1} for the samples annealed at 200 and 300°C .⁷⁴

The IR spectra of *p*-Si have been investigated under various experimental conditions by several authors.^{70,75-77} Reports about the effect of chemical and thermal oxidation show changes in the IR spectra of *p*-Si which are almost identical to the ones described above for siloxene.⁷⁸

The IR spectra of siloxene (Fig. 14) further show that

hydrogen is easily evolved from the material at temperatures above about 400 °C. This is corroborated by the effusion curves of Fig. 16. For these measurements the samples were placed in an evacuated cell, and the partial pressure of hydrogen was measured with a mass spectrometer while the temperature was increased linearly in time. The main effusion for siloxene occurs as a sharp peak at about 400 °C.⁷⁹ A similar peak is observed for *p*-Si but with an additional high-temperature peak at about 540 °C. We gain some insight into the origin of these two peaks by comparing the results of siloxene and *p*-Si with *a*-Si:H and with crystalline Si (*c*-Si) which has been exposed to a H₂ plasma at 20 °C and 250 °C (Fig. 16). It is well known that the surface of crystalline Si in a H₂ plasma at room temperature is passivated by hydrogen.^{80,81} Clusters of hydrogen are present on the Si surface which can desorb as H₂ molecules at temperatures of about 400 °C. If silicon is exposed to the H₂ plasma at elevated temperatures (250 °C), hydrogen diffuses into the material forming isolated Si-H bonds. Somewhat higher temperatures near 540 °C are required to break these bonds and effuse molecular H₂ from the silicon. Isolated Si-H bonds, rather than H clusters, are also present in hydrogenated *a*-Si:H leading to a similar (high-temperature) peak in the effusion curve. The free bonds of the silicon atoms in the Si₆ rings and the Si planes in siloxene are passivated with hydrogen similar to the surface of crystalline Si, leading to the 400 °C peak in the effusion curves. In porous Si, however, either some of the hydrogen has diffused into the Si skeleton or is bound in a way similar to *a*-Si:H, giving rise to the additional 540 °C peak.

As a result of the effusion of hydrogen, the Si-H modes

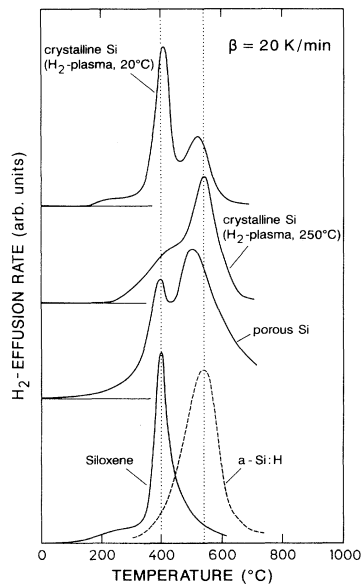


FIG. 16. Hydrogen-effusion curves of siloxene and porous silicon. The curves of amorphous silicon and crystalline silicon exposed to a H₂ plasma at 20 °C and 250 °C are shown for comparison (see text for details).

of the IR spectra in Fig. 14 and the O-H vibrations around 3400 cm⁻¹ are drastically reduced for samples annealed above 300 °C, and the remaining substoichiometric oxide SiO_x leads to the strong Si-O-Si vibrations around 1100 cm⁻¹ (stretch) and 460 cm⁻¹ (bend). This is again in good agreement with the Raman data, where a broad 470-cm⁻¹ mode appeared for the samples annealed above 400 °C. The effusion of hydrogen is also accompanied by a simultaneous increase of paramagnetic defects, detected by electron spin resonance.⁸² These defects act as nonradiative recombination centers and should be taken into account in explaining the reduction in PL intensity after annealing to temperatures above 400 °C.

In analogy to the Raman experiments discussed above, we also monitored the structural changes of siloxene under intense illumination by IR spectroscopy (Fig. 17). As in the discussion of Figs. 1(a)–1(c), the changes in the IR spectra after intense illumination and after annealing at moderate temperatures (200 °C in this case) are very similar. The 520-cm⁻¹ mode (an indication of Si-planes in siloxene) and the 645-cm⁻¹ mode vanish, and modes at 845 cm⁻¹, 870 cm⁻¹ become stronger. In addition, the indications of increasing insertion of oxygen into the Si planes, discussed above as a result of the thermal annealing, are clearly visible in both the annealed and the irradiated sample: the double peak structure at around 1100 cm⁻¹ from Si-O-Si stretch vibrations, the 460-cm⁻¹ Si-O-Si bend mode, and the O-Si-H vibrations at 2200 cm⁻¹ and 2250 cm⁻¹. Similar studies of the effect of illumination on the IR spectra of porous silicon have been performed by Mauckner, Thonke, and Sauer. Their results⁶¹ are very similar to those just discussed for siloxene. Collins *et al.* have correlated the decrease of the PL efficiency upon UV irradiation with optically induced hydrogen desorption.⁸³ They found that the rate

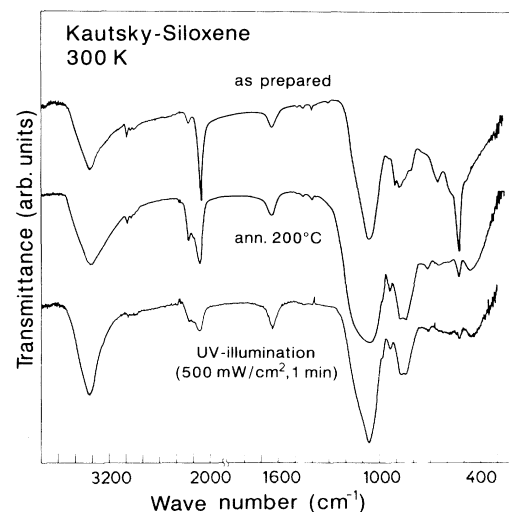


FIG. 17. Room-temperature infrared transmittance of Kautsky siloxene as prepared (upper trace), annealed at 200 °C (middle trace), and after UV illumination in ambient air (lower trace).

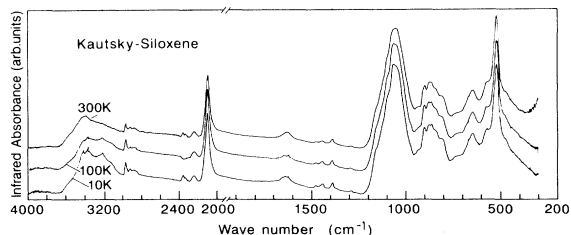


FIG. 18. Infrared absorption spectra of Kautsky siloxene at 10 K (lower trace), 100 K (middle trace), and 300 K (upper trace).

at which the luminescence intensity degrades increases rapidly when the illumination energy exceeds a threshold near 3 eV.⁸³

In order to follow the evolution of the vibrational properties of siloxene at low temperatures, IR spectra of the as-prepared Kautsky siloxene were taken at temperatures between 10 K and 300 K. Figure 18 shows three spectra at 10 K, 100 K, and 300 K. Within the uncertainty of the measurement, these spectra show no anomalous behavior of the vibrations at low temperatures as has been reported for *p*-Si by Feng, Payne, and Perkowitz⁸⁴ Since the thermal conductivity of *p*-Si is quite low, temperature-dependent measurements require care to avoid sample heating due to the exciting light. In the IR spectra of Fig. 18, the incident intensities are so small that we can exclude any temperature effects from the incident light.

V. CONCLUSIONS

The Raman and infrared transmission spectra of various forms of siloxene ($\text{Si}_6\text{O}_3\text{H}_6$) have been analyzed to determine the structural properties of these materials. Three models have been proposed in the literature:

Si_6 rings interconnected by oxygen, linear Si-H chains crosslinked by O, and Si planes terminated by H and OH. Our measurements suggest that siloxene usually consists of a mixture of these configurations, depending on the thermal, chemical, and irradiation treatment. Siloxene produced according to Kautsky's recipe displays blue-green luminescence and consists mainly of the Si(111)-plane structure which is unstable against heating or illumination in oxygen. Oxygen (from the OH ligands) is inserted into the Si planes by thermal activation (annealing below 400 °C) or, to some degree, by allowing oxygen in the manufacturing process (Wöhler's recipe for siloxene). The fragmentation of the Si planes leads to the formation of Si structures (Si_6 rings, Si chains, etc.) which are isolated from each other by oxygen bridges. Such siloxene displays luminescence in the red region and shows various properties similar to electrochemically anodized porous silicon. In particular the Raman and infrared transmission spectra are almost identical over the entire frequency range from 300 cm^{-1} to 4000 cm^{-1} . The efficiency of the photoluminescence of porous Si and siloxene is orders of magnitude larger than in any other comparable substance. We propose a similar mechanism of the luminescence in porous silicon and siloxene: optical recombination in two-, one-, and zero-dimensional Si structures [Si(111) planes, Si_6 rings, etc.], which are passivated by ligands and electrically isolated (e.g., by oxygen bridges).

ACKNOWLEDGMENTS

Technical assistance by M. Siemers, P. Wurster, H. Hirt, and P. Andler is gratefully acknowledged. We want to thank A. Breitschwerdt for the IR measurements, and V. Lehmann and J. Köhler for performing the x-ray-diffraction studies. We also would like to thank P. England, V. Lehmann, and W. Lang for providing *p*-Si samples.

*Permanent address: Technical University, Budapest H-1521, Hungary.

¹M.S. Hybertson, in *Light Emission from Silicon*, edited by S.S. Iyer, R.T. Collins, and L.T. Canham, MRS Symposium Proceedings No. 256 (Materials Research Society, Pittsburgh, 1992), p. 179.

²G.D. Sanders and Y.C. Chang, *Phys. Rev. B* **45**, 9202 (1992).

³M.S. Brandt, H.D. Fuchs, A. Höpner, M. Rosenbauer, M. Stutzmann, J. Weber, M. Cardona, and H.J. Queisser, MRS Symposia Proceedings No. 262 (Materials Research Society, Pittsburgh, 1993), p. 849.

⁴L.T. Canham, *Appl. Phys. Lett.* **57**, 1046 (1990); *Physics World* **5**, 41 (1992).

⁵V. Lehmann and U. Gösele, *Appl. Phys. Lett.* **58**, 856 (1991).

⁶D.R. Turner, *J. Electrochem. Soc.* **105**, 402 (1958).

⁷E. Bustarret, M. Ligeon, and L. Ortega, *Solid State Commun.* **83**, 461 (1992).

⁸P. McCord, S. Yau, and A.J. Bard, *Science* **257**, 68 (1992).

⁹E.A. Meulenkamp, P.M.M.C. Bressers, and J.J. Kelly, *Appl. Surf. Sci.* **64**, 283 (1993).

¹⁰J.K.M. Chun, A.B. Bocarsly, T.R. Cottrell, J.B. Benzinger, and J.C. Yee, in *Microcrystalline Semiconductors—Materials Science and Devices*, edited by Y. Aoyagi, L. T. Canham, P. M. Fauchet, I. Shimizu, and C. C. Tsai, MRS Symposia Proceedings No. 283 (Materials Research Society, Pittsburgh, 1993).

¹¹J.L. Coffey, S.C. Lilley, R.A. Martin, and L.A. Files-Sesler, in *Microcrystalline Semiconductors—Materials Science and Devices*, edited by Y. Aoyagi, L. T. Canham, P. M. Fauchet, I. Shimizu, and C. C. Tsai, MRS Symposium Proceedings No. 283 (Materials Research Society, Pittsburgh, 1993).

¹²H.D. Fuchs, M.S. Brandt, M. Stutzmann, and J. Weber, in *Light Emission from Silicon* (Ref. 1), p. 159; M.S. Brandt, H.D. Fuchs, M. Stutzmann, J. Weber, and M. Cardona, *Solid State Commun.* **81**, 307 (1992).

¹³J.C. Adams, T.P. Pearsall, J.E. Wu, B.Z. Noshov, C. Aw, and J.C. Patton, *J. Appl. Phys.* **71**, 4470 (1992).

¹⁴A.G. Cullis and L.T. Canham, *Nature* **353**, 335 (1991).

- ¹⁵M. Stutzmann, J. Weber, M.S. Brandt, H.D. Fuchs, M. Rosenbauer, P. Deak, A. Höpner, and A. Breitschwerdt, *Adv. Solid State Phys.* **32**, 179 (1992).
- ¹⁶*Light Emission from Silicon* (Ref. 1).
- ¹⁷S.M. Prokes, J.A. Freitas Jr., and P.C. Searson, *Appl. Phys. Lett.* **60**, 3295 (1992).
- ¹⁸F. Wöhler, *Lieb. Ann.* **127**, 275 (1863).
- ¹⁹H. Kautsky and H. Zocher, *Z. Phys.* **9**, 267 (1922).
- ²⁰A. Weiss, G. Beil, and H. Meyer, *Z. Naturforsch.* **34b**, 25 (1979).
- ²¹J.R. Dahn, B.M. Way, E. Fuller, and J.S. Tse, *Bull. Am. Phys. Soc.* **38**, 56 (1993).
- ²²P.C. Pearson, *Appl. Phys. Lett.* **59**, 832 (1991).
- ²³S. Fahy and D.R. Hamann, *Phys. Rev. B* **41**, 7587 (1990).
- ²⁴J.F. Morar and M. Wittmer, *Phys. Rev. B* **37**, 2618 (1988).
- ²⁵M.S. Brandt, A. Breitschwerdt, H.D. Fuchs, M. Rosenbauer, M. Stutzmann, and J. Weber, *Appl. Phys. A* **54**, 567 (1992).
- ²⁶H.D. Fuchs, M. Stutzmann, M.S. Brandt, M. Rosenbauer, and M. Cardona, *Phys. Scr.* **T45**, 309 (1992).
- ²⁷*Gmelins Handbuch der Anorganischen Chemie, Silicium, Teil B*, edited by R.J. Meyer, E.H.E. Pietsch, and A. Kottowski (Verlag Chemie, Weinheim, 1959).
- ²⁸P. Deák, M. Rosenbauer, M. Stutzmann, J. Weber, and M.S. Brandt, *Phys. Rev. Lett.* **69**, 2531 (1992).
- ²⁹H. Kautsky and G. Herzberg, *Z. Anorg. Chemie* **139**, 135 (1924).
- ³⁰E. Hengge, *Chem. Ber.* **95**, 648 (1962).
- ³¹H. Ubara, T. Imura, A. Hiraki, I. Hirabayashi, and K. Morigaki, *J. Non-Cryst. Solids* **59 & 60**, 641 (1983).
- ³²M. Cardona, *Phys. Status Solidi B* **118**, 463 (1983).
- ³³G. Lucovsky and W.B. Pollard, in *Hydrogenated Amorphous Silicon II*, edited by J.D. Joannopoulos and G. Lucovsky (Springer, Berlin, 1984), p. 301.
- ³⁴D.J. Wolford, J.A. Reimer, and B.A. Scott, *Appl. Phys. Lett.* **42**, 369 (1983).
- ³⁵N. Matsumoto, S. Furukawa, and K. Takeda, *Solid State Commun.* **53**, 881 (1985).
- ³⁶P. Vora, S.A. Solin, and P. John, *Phys. Rev. B* **29**, 3423 (1984).
- ³⁷E. Sacher, *Philos. Mag.* **51**, 295 (1985).
- ³⁸G.W. Bethke and M.K. Wilson, *J. Chem. Phys.* **26**, 1107 (1957).
- ³⁹S.R. Goodes, T.E. Jenkins, M.I.J. Beale, J.D. Benjamin, and C. Pickering, *Semicond. Sci. Technol.* **3**, 483 (1988).
- ⁴⁰J.C. Tsang, M.A. Tischler, and R.T. Collins, *Appl. Phys. Lett.* **60**, 2279 (1992).
- ⁴¹R. Tsu, H. Shen, and M. Dutta, *Appl. Phys. Lett.* **60**, 112 (1992).
- ⁴²H. Richter, Z.P. Wang, and L. Ley, *Solid State Comm.* **39**, 625 (1981).
- ⁴³I.H. Campbell and P.M. Fauchet, *Solid State Commun.* **58**, 739 (1986).
- ⁴⁴A.K. Sood, K. Jayaram, D. Victor, and S. Muthu, *J. Appl. Phys.* **72**, 4963 (1992).
- ⁴⁵G. Kanellis, J.F. Morhange, and M. Balkanski, *Phys. Rev. B* **21**, 1543 (1980).
- ⁴⁶H. Tanino, H. Kawanami, and H. Matsuhata, *Appl. Phys. Lett.* **60**, 1978 (1992).
- ⁴⁷L.L. Boyer, E. Kaxiras, J.L. Feldmann, J.Q. Broughton, and M.J. Mehl, *Phys. Rev. Lett.* **67**, 715 (1991).
- ⁴⁸E. Hengge and K. Pretzer, *Chem. Ber.* **96**, 470 (1963).
- ⁴⁹G. Herzberg in *Molecular Spectra and Molecular Structure* (Van Nostrand Reinhold, New York, 1945), Vol. 2.
- ⁵⁰R.M. Martin, *Phys. Rev. B* **1**, 4005 (1970).
- ⁵¹T.R. Gilson and P.J. Hendra, *Laser Raman Spectroscopy* (Wiley, London 1970).
- ⁵²S. Go, H. Bilz, and M. Cardona, *Phys. Rev. Lett.* **34**, 580 (1975).
- ⁵³H. Kriegmann, *Z. Anorg. Allg. Chem.* **298**, 232 (1959).
- ⁵⁴F.L. Galeener, R.A. Barrio, E. Martinez, and R.J. Elliott, *Phys. Rev. Lett.* **53**, 2429 (1984).
- ⁵⁵R.J. Hemley, H.K. Mao, P.M. Bell, and B.O. Mysen, *Phys. Rev. Lett.* **57**, 747 (1986).
- ⁵⁶C. Fiori (private communication).
- ⁵⁷C. Fiori and R.A.B. Devine, *Phys. Rev. B* **33**, 2972 (1986); C. Fiori and R.A.B. Devine, *Phys. Lett.* **52**, 2081 (1984); O. Joubert, G. Hollinger, C. Fiori, R.A.B. Devine, P. Paniez, and R. Pantel, *Phys. J. Appl. Phys.* **69**, 6647 (1991).
- ⁵⁸H.C. Chen, W. Wang, K.N. Manjularani, L.C. Snyder, and X.L. Zheng (Ref. 1), p. 197.
- ⁵⁹S. Shih, C. Tsai, K.-H. Li, H. Jung, J.C. Campbell, and D.L. Kwong, *Appl. Phys. Lett.* **60**, 633 (1992).
- ⁶⁰J.C. Vial, A. Bsiesy, F. Gaspard, R. Hérino, M. Ligeon, F. Muller, R. Romestain, and R.M. MacFarlane, *Phys. Rev. B* **45**, 14171 (1992).
- ⁶¹G. Mauckner, K. Thonke, and R. Sauer (unpublished).
- ⁶²H. Takagi, O. Ogawa, Y. Yamazaki, A. Ishizaki, and T. Nakagiri, *Appl. Phys. Lett.* **56**, 2379 (1990).
- ⁶³M.A. Tischler, R.T. Collins, J.H. Stathis, and J.C. Tsang, *Appl. Phys. Lett.* **60**, 639 (1992).
- ⁶⁴P.M. Fauchet, in *Light Scattering in Semiconductor Structures and Superlattices*, edited by D.J. Lockwood and J.F. Young (Plenum, New York, 1990).
- ⁶⁵K. Hassler, E. Hengge, and D. Kovar, *Spectrochim. Acta A* **34**, 1193 (1978).
- ⁶⁶E. Wiberg and W. Simmler, *Z. Anorg. Allg. Chem.* **283**, 401 (1956).
- ⁶⁷J.C. Knights, R.A. Street, and G. Lucovsky, *J. Non-Cryst. Solids* **35**, 279 (1980).
- ⁶⁸B.G. Yacobi, R.W. Collins, G. Moddel, P. Viktorovitch, and W. Paul, *Phys. Rev. B* **24**, 5907 (1981).
- ⁶⁹M.A. Tischler and R.T. Collins, *Solid State Commun.* **84**, 819 (1992).
- ⁷⁰Y.H. Xie, W.L. Wilson, F.M. Ross, J.A. Mucha, E.A. Fitzgerald, J.M. Macaulay, and T.D. Harris, *Appl. Phys. Lett.* **71**, 2403 (1992).
- ⁷¹N. Wright and M.J. Hunter, *J. Am. Chem. Soc.* **69**, 803 (1947).
- ⁷²M. Stavola, *Appl. Phys. Lett.* **44**, 514 (1984); B. Pajot, H.J. Stein, B. Cales, and C. Naud, *J. Electrochem. Soc.* **132**, 3034 (1985).
- ⁷³Y.J. Chabal, in *Hydrogen in Semiconductors: Bulk and Surface Properties*, edited by M. Stutzmann and J. Chevallier (North-Holland, Amsterdam 1991).
- ⁷⁴G. Lucovsky, J. Yang, S.S. Chao, J.E. Tyler, and W. Czuby, *Phys. Rev. B* **28**, 3225 (1983).
- ⁷⁵C.Tsai, K.-H. Li, D.S. Kinosky, R.-Z. Qian, T.-C. Hsu, J.T. Irby, S.K. Banerjee, A.F. Tasch, J. C. Campbell, B.K. Hance, and J.M. White, *Appl. Phys. Lett.* **60**, 1700 (1992).
- ⁷⁶W. Theiss, P. Grosse, H. Mündler, H. Lüth, R. Hérino, and M. Ligeon, *Appl. Surf. Sci.* **63**, 240 (1993).
- ⁷⁷Y. Ochiai, N. Ookubo, H. Watanabe, S. Matsui, Y. Mochizuki, H. Ono, S. Kimura, and T. Ichihashi, *Jpn. J. Appl. Phys.* **31**, L560 (1992).
- ⁷⁸A. Nakajima, T. Itakura, S. Watanabe, and N. Nakayama, *Appl. Phys. Lett.* **61**, 46 (1992), and references therein.
- ⁷⁹R.W. Hardeman, M.I.J. Beale, D.B. Gasson, J.M. Keen,

- C. Pickering, and D.J. Robbins, Surf. Sci. **152/153**, 1051 (1985).
- ⁸⁰D.B. Fenner, D.K. Biegelsen, and R.D. Bringans, J. Appl. Phys. **66**, 419 (1989).
- ⁸¹Y.J. Chabal, G.S. Higashi, and S.B. Christman, Phys. Rev. B **28**, 4472 (1983).
- ⁸²M.S. Brandt and M. Stutzmann, Appl. Phys. Lett. **61**, 2569 (1992).
- ⁸³R.T. Collins, M.A. Tischler, and J.H. Strathis, Appl. Phys. Lett. **61**, 1649 (1992).
- ⁸⁴Z.C. Feng, J.R. Payne, and S. Perkowitz, Bull. Am. Phys. Soc. **37**, 564 (1992).

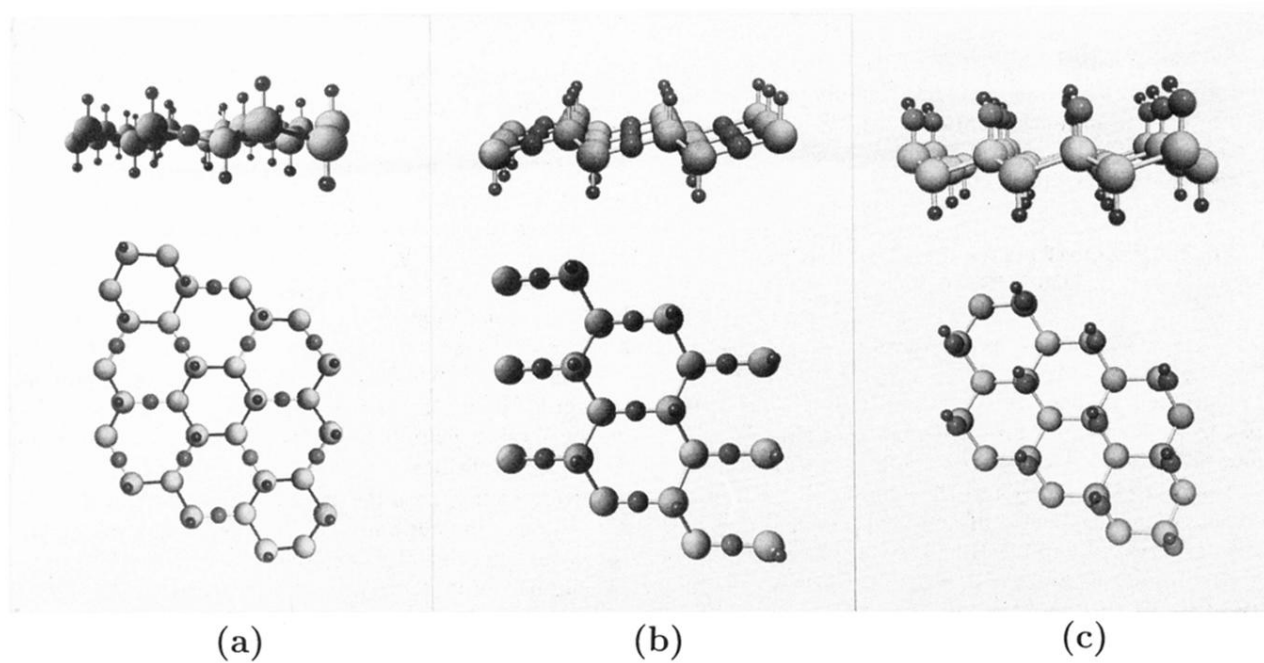


FIG. 3. Structural model of the different modifications of stoichiometric siloxene ($\text{Si}_6\text{O}_3\text{H}_6$): (a) Si_6 rings and (b) Si chains interconnected via oxygen bridges and terminated by hydrogen, (c) Si planes terminated by H and OH. Light atoms symbolize Si, small dark atoms hydrogen and larger dark atoms oxygen.